

# Beryllium-10 surface exposure dating of glacial successions in the Central Alaska Range

JASON M. DORTCH,<sup>1\*</sup> LEWIS A. OWEN,<sup>1</sup> MARC W. CAFFEE,<sup>2</sup> DEWEN LI<sup>3</sup> and THOMAS V. LOWELL<sup>1</sup>

<sup>1</sup> Department of Geology, University of Cincinnati, Cincinnati, Ohio, USA

<sup>2</sup> Department of Physics, Purdue University, West Lafayette, Indiana, USA

<sup>3</sup> China Earthquake Disaster Prevention Center, Beijing, China

Dortch J. M., Owen L. A., Caffee M. W., Li D., Lowell T. V. 2010. Beryllium-10 surface exposure dating of glacial successions in the Central Alaska Range. *J. Quaternary Sci.*, Vol. 25 pp. xxx–xxx. ISSN 0267-8179.

Received 19 September 2009; Revised 2 February 2010; Accepted 15 March 2010

**ABSTRACT:** Glacial landforms and outwash terraces in the Nenana River valley, Reindeer Hills and Monahan Flat in the central Alaska Range were dated with 60 <sup>10</sup>Be exposure ages to determine the timing of Late Pleistocene glaciation. In the Nenana River valley, glaciation occurred at 104–180 ka (Lignite Creek glaciation), ca. 55 ka (Healy glaciation), and ca. 16 ka (Carlo Creek phase); glaciers retreated in the Reindeer Hills and Monahan Flat by ca. 14 ka and ca. 13 ka, respectively. The Carlo Creek moraine is similar in age to at least six other moraines in the Alaska Range, Ahklun Mountains and Brooks Range. The new data suggest that post-depositional geological processes limit the usefulness of <sup>10</sup>Be methods to the latter part (≤60 ka) of the late Quaternary in central Alaska. Ages on Healy and younger landforms cluster well, with the exception of Riley Creek moraines and Monahan Flat-west sites, where boulders were likely affected by post-depositional processes. Copyright © 2010 John Wiley & Sons, Ltd.

Supporting information may be found in the online version of this article.

**KEYWORDS:** glaciation; surface exposure dating; Alaska Range; geochronology; moraine.

## Introduction

Reconstructions of palaeoenvironmental change with proxy data such as the glacial geological record enable the development and testing of predictive models for future environmental change (LIGA Members, 1991). The most severe environmental changes are expected to occur in high-latitude regions such as Alaska (Arendt *et al.*, 2002; IPCC, 2007). Fortunately, these regions contain abundant glacial geological evidence that may be used to reconstruct palaeoclimatic conditions, which in turn can be used to test predictive models. Determining the timing of glaciation based on glacial geological evidence is challenging, but newly developing dating methods such as terrestrial cosmogenic nuclide dating is helping to define the ages of glacial successions (Gosse and Phillips, 2001). The moraines and terraces in the central Alaska Range comprise some of the most detailed Pleistocene records of glaciation in Alaska (Wahrhaftig, 1958; Thorson and Hamilton, 1976; Ten Brink and Waythomas, 1985; Thorson, 1986). However, these landforms have not been previously dated in detail (Briner and Kaufman, 2008). Using <sup>10</sup>Be terrestrial cosmogenic nuclide surface exposure dating (<sup>10</sup>Be dating), we examine and develop a quantitative chronology for glaciation in the central Alaska Range, focusing

on the Nenana River valley, Reindeer Hills and Monahan Flat areas (Fig. 1). This chronology can be used by future researchers to develop detailed palaeoenvironmental histories for the region to aid in modelling environmental change. Furthermore, geologists working on tectonics in this seismically active region can utilise our chronology to help determine rates and magnitudes of crustal displacement for seismic hazard mitigation (Matmon *et al.*, 2006).

## Regional setting

The Alaska Range in south-central Alaska is a convex northern mountain belt that stretches E–W for ~950 km and is 80–200 km wide (Fig. 1). The relief is impressive, rising from forelands <1000 m above sea level (a.s.l.) to the highest peak, Denali (formally known as Mount McKinley) in North America, at 6194 m a.s.l. The central Alaska Range was produced by the collision of an island-arc assemblage with the former North American continental margin, which has progressively deformed throughout the late Mesozoic and Cenozoic, and is still undergoing active surface deformation (Ridgway *et al.*, 2002; Eberhart-Phillips *et al.*, 2003; Matmon *et al.*, 2006). The range crest separates the maritime climate of southern Alaska from the colder continental climate of the Alaskan interior (Capps<sup>Q2</sup>, 1940). The Alaska Range marks the northern limit of the Cordilleran Ice Sheet, but outlet glaciers and isolated alpine

\*Correspondence to: J. M. Dortch, Department of Geology, University of Cincinnati, 500 Geo/Physics Building, Cincinnati, OH 45220, USA. E-mail: dortchjm@mail.uc.edu



Journal of Quaternary Science

61  
62  
63  
64  
65  
66  
67  
68  
69  
70  
71  
72  
73  
74  
75  
76  
77  
78  
79  
80  
81  
82  
83  
84  
85  
86  
87  
88  
89  
90  
91  
92  
93  
94  
95  
96  
97  
98  
99  
100  
101  
102  
103  
104  
105  
106  
107  
108  
109  
110  
111  
112  
113  
114  
115  
116  
117  
118  
119  
120



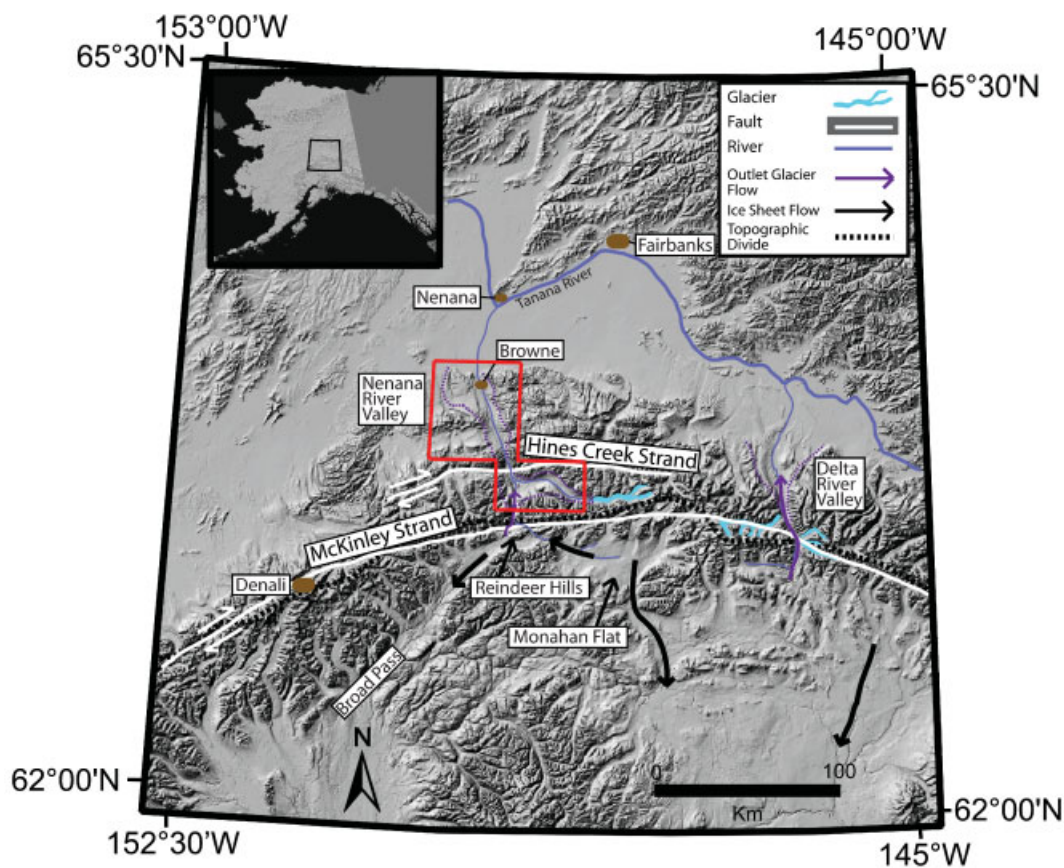


**Figure 1** Digital elevation model for the central Alaska Range (using USGS seamless data at <http://seamless.usgs.gov/>). The topographic divide separates drainage that flows south via Broad Pass and the Monahan Flat to the Cook Inlet and the Gulf of Alaska from drainage that flows north to the Bering Sea via the Tanana River. There are two notable exceptions: the Nenana River and the Delta River, which head south of the divide and flow north across the Alaska Range to the Tanana River. Red box shows location of Fig. 2. Ice flow directions are from Wahrhaftig (1958) and Hamilton and Thorson (1983). Fault traces are taken from Warhaftig (1958), Thorson (1986) and [Hickman<sup>Q1</sup>](#) (1977)

glaciers on the northern slopes of the Alaska Range advanced northward into the foreland (Wahrhaftig, 1958; Hamilton and Thorson, 1983).

## Study areas

Three regions were examined in the central Alaska Range: the Nenana River valley on the northern side of the Alaska Range, and Reindeer Hills and the Monahan Flat of the southern side (Fig. 1).

The Nenana River valley traverses the central and northern part of the Alaska Range and contains a well-preserved succession of moraines and terraces (Wahrhaftig, 1958; Fig. 2). The bedrock comprises the Birch Creek Schist and the Cantwell Formation, which includes conglomerate, sandstone, shale, argillite and volcanic rocks (Wahrhaftig, 1958; Thorson, 1986). The head of the Nenana River valley forms a deep U-shaped corridor (~15 km long, 3.5 km wide and 1.5 km deep) that was deepened by north-flowing outlet glaciers from the Cordilleran Ice Sheet that coalesced with the local Yanert Glacier (Hamilton and Thorson, 1983; Thorson and Bender, 1985; Thorson, 1986). North of the confluence, the Nenana River valley narrows to form a glacial trough ~2.5 km wide and ~1.5 km deep (Thorson, 1986). The valley contains numerous well-preserved north-sloping glacial trimlines recording successive advances and is wider (7–10 km) north of the glacial trough as it traverses the more easily eroded substrate that comprises the Nenana Gravel (Wahrhaftig, 1958; Thorson, 1986).

In the Nenana River valley, Wahrhaftig (1958) and Thorson (1986) identified at least seven sets of moraines and assigned these to Pleistocene glaciations, which they termed the Taklanika (oldest), Browne, Bear Creek, Lignite Creek (Wahrhaftig's, 1958, original Dry Creek advance), Healy, Riley Creek 1 and 2 phases and Carlo Creek phase (youngest; Fig. 2 and Table 1). Numerical dating of these events is limited to seven radiocarbon ages on the Riley Creek 1 and 2 and Carlo Creek glacial landforms, constraining them to the late Wisconsin glaciation, and one tephra ( $175 \pm 12$  ka to  $378 \pm 67$  ka using thermoluminescence (TL) and  $^{40}\text{Ar}/^{39}\text{Ar}$  method, respectively) in the Lignite Creek moraine (Wahrhaftig, 1958; Ten Brink and Waythomas, 1985; Begét and Keskinen, 1991; Reger *et al.*, 1996). Additional moraines are located in the Eight Mile Lake region (Fig. 2), but their relationship to the Nenana moraine sequence is unresolved (Thorson, 1986).

The Reindeer Hills, near the town of Windy on the southern side of the Alaska Range, is an 8 km long ridge that rises ~700 m above the valley floor to >1300 m a.s.l. (supporting information, Figs 1SI and 2SI). The hills comprise schist and metasedimentary rocks. Five glaciated benches flank the Reindeer Hills, sloping 1–2° to the west. Wahrhaftig (1958) suggested that glaciers covered the Reindeer Hills, leaving only the uppermost peaks as nunataks during the Riley Creek glaciation.

The Monahan Flat is a glaciated lowland at an altitude of ~800 m a.s.l. and is located 30 km east of the Reindeer Hills on the southern side of the Alaska Range; it stretches for ~40 km and is ~24 km wide. During glacial times the Nenana, West Fork and Susitna glaciers advanced into this lowland, flowing west towards the Reindeer Hills region and through Broad Pass (supporting information, Fig. 2SI; Wahrhaftig, 1958).

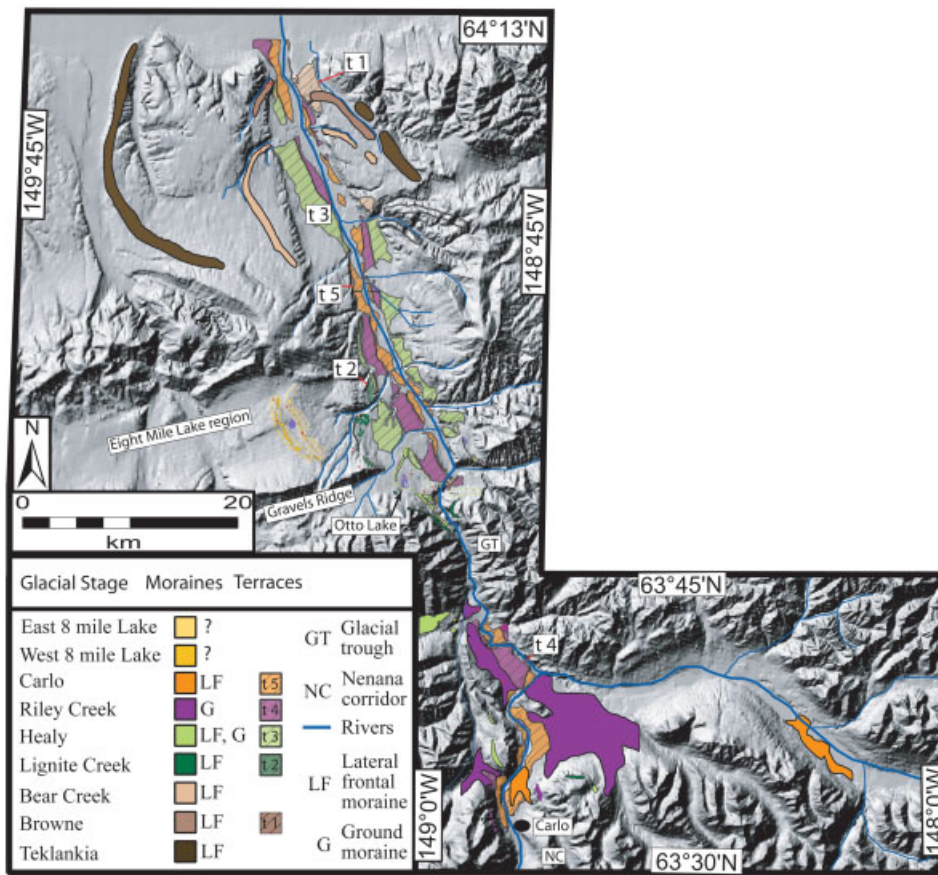


**Figure 2** Digital elevation model (using USGS seamless data at <http://seamless.usgs.gov/>), showing the location of moraines and outwash terraces in the Nenana valley (see Fig. 1 for location). Moraines and outwash terraces for each glacial stage are listed in chronostratigraphic order in the legend except for the Eight Mile Lake glacial stage moraines, whose morphostratigraphic relationship with the other landforms is not known with any certainty (Thorson, 1986)

## Methods

We used the mapping of Wahrhaftig (1958), Thorson and Hamilton (1976) and Thorson (1986) as a framework for our study to identify Lignite Creek (most extensive), Healy, Riley Creek 1, Riley Creek 2, and the Carlo Creek glacier landforms and sediments. Thorson and Hamilton (1976) recognised the Riley Creek 1, Riley Creek 2, and the Carlo Creek landforms and deposits as belonging to the late Wisconsin glaciation (Marine Isotope Stage (MIS) 2). The mapping of moraines and outwash terraces by Thorson and Hamilton (1976) was verified in the field, aided by aerial photography, a 2° National Elevation Dataset digital elevation model (DEM) (obtained from US Geological Survey, 2007) and Landsat-7

satellite imagery (University of Maryland; <http://glcf.umd.edu/data>). Sediments were described and logged using the methods and nomenclature of Evans and Benn (2004).

Thirty-two samples from boulders and glacially polished bedrock for <sup>10</sup>Be dating were located by traversing the length of each moraine, drumlin and regions of polished bedrock for each glaciation (Lignite Creek through Carlo Creek). An additional 23 samples were collected from glacial landforms south of the range divide (Reindeer Hills and Monahan Flat) to obtain rates of ice retreat after the last glacial. Finally, five samples for a <sup>10</sup>Be depth profile were collected from a gravel pit excavated to 2 m depth in the Lignite Creek moraine. The sedimentary structures were plotted onto graphic sedimentary logs (supporting information, Fig. 3SI).

**Table 1** Glacial stages in the Nenana River valley, their assigned ages as defined by previous researchers and revised suggested ages based on this study

Glacial stage (morphostratigraphic order)	Wahrhaftig (1958)	Thorson (1986)	Beget <sup>Q3</sup> et al. (1991)	Range of ages (ka)	Weighted mean (ka)	This study
Monahan Flat east	—	—	—	13–14	13.2 ± 2.2	ca. 13 ka
Monahan Flat west	—	—	—	1.3–34	—	—
Reindeer Hills	—	—	—	12–18	14.3 ± 1.2	ca. 14 ka
Carlo Creek <sup>a</sup>	Late Wisconsin	—	—	13–22	16.0 ± 1.8	ca. 16 ka
Riley Creek 2 event	Late Wisconsin	—	—	9–61	11.0 ± 2.9	—
Riley Creek 1 event	Late Wisconsin	Late Wisconsin	Late Wisconsin	1–10	—	—
Healy	No comment	>Late Wisconsin	ca. 60 ka	28–59	54.6 ± 3.5	ca. 55 ka
Lignite Creek	Coupled with Healy stage	Separate advance	ca. 140 ka	13–104	—	104–180 ka

<sup>a</sup> Referred to by Thorson (1986) as the Carlo Readvance.

1 Sampling boulders where evidence of exhumation and/or  
 2 slope failure was apparent was avoided in all study locations.  
 3 The location, geomorphic setting, lithology, size, shape and  
 4 weathering features were recorded for each sample (Table 2;  
 5 supporting information, Table 1SI). Quartz-rich boulders >1 m  
 6 high were chosen for sampling when possible to reduce the  
 7 possibility of shielding for significant periods by snow, moss or  
 8 former loess cover (Fig. 3). The upper 1–5 cm of each boulder  
 9 was sampled with hammer and chisel. Topographic shielding  
 10 was determined by measuring the inclination from the boulder  
 11 to the top of the surrounding horizon. Multiple samples (ranging  
 12 from 3 to 13) were collected from each glacial limit (Fig. 4).  
 13 In addition, two boulders (Ala 126 A/B and Ala 137 A/B) were  
 14 sampled twice to check for the effects of differential weathering  
 15 on exposure age (Fig. 3(D)).

16 Isolation of quartz and chemistry followed the methods of  
 17 Kohl and Nishiizumi (1992) and is described in detail in Dortch  
 18 *et al.* (2009). SPEX beryllium standard (trace [ICP/ICP-MS<sup>Q5</sup>](#)  
 19 grade) at 1000  $\mu\text{g mL}^{-1}$  in 2%  $\text{HNO}_3$  was used for all samples  
 20 and blanks. Ten chemical blanks were processed and had a  
 21 weighted mean  $^9\text{Be}/^{10}\text{Be}$  ratio of  $3.91 \times 10^{-14} \pm 0.58 \times 10^{-14}$ .  
 22 The Purdue Rare Isotope Measurement (PRIME) Laboratory  
 23 accelerator mass spectrometer was calibrated using standard  
 24 200500020 from KN Standard Be 0152 with a  $^9\text{Be}/^{10}\text{Be}$  ratio of  
 25  $9465 \times 10^{-15}$ . All  $^9\text{Be}/^{10}\text{Be}$  ratios were converted to the revised  
 26 ICN of Nishiizumi *et al.* (2007), which is assumed to be the  
 27 most correct standard and requires a production rate of 4.5  
 28  $^{10}\text{Be}$  atoms  $\text{a}^{-1}$  and a half-life of 1.36 Ma for age calculation  
 29 (PRIME Laboratory, 2007). Because the samples were measured  
 30 on the PRIME Laboratory accelerator mass spectrometer, all  
 31 reported  $^{10}\text{Be}$  ages were calculated using the (PRIME)  
 32 Laboratory Rock Age Calculator with the Lal (1991)/Stone  
 33 (2000) scaling scheme, which accounts for spallogenic and fast/  
 34 slow muogenic  $^{10}\text{Be}$  production (<http://www.physics.purdue.edu/primelab/News/news0907.php>).

## 35 $^{10}\text{Be}$ ages

36  $^{10}\text{Be}$  ages are shown in Fig. 4 and Table 2. These are not  
 37 corrected for boulder weathering. There are two sets of factors  
 38 that affect  $^{10}\text{Be}$  ages: uncertainties associated with the  
 39  $^{10}\text{Be}$  production rate, scaling factors, geomagnetic corrections  
 40 and accelerator mass spectrometric (AMS) measurements  
 41 combined with sample preparation and carrier uncertainties;  
 42 and those involving geological processes, including shielding  
 43 by sediment/snow cover, exhumation of bedrock surfaces or  
 44 boulders, stability of boulders and inheritance of  $^{10}\text{Be}$ . Scaling  
 45 uncertainties are not a major concern within our study area  
 46 since all our locations are at high latitude and relatively low  
 47 altitude (see KN ages in Table 2; Balco *et al.*, 2008). Although  
 48 there is uncertainty in absolute production rates, our samples  
 49 are from the same geographical area so age comparisons  
 50 between samples are isolated from production rate uncertain-  
 51 ties. AMS measurement, sample preparation, and age calcu-  
 52 lation uncertainties can have a maximum of 50% error (Ala-19)  
 53 in our dataset, but is more typically 10%. The large range in  
 54  $^{10}\text{Be}$  ages, such as those from the Lignite Creek moraine, is  
 55 attributed to geological processes. The greatest uncertainties in  
 56 our dataset are those associated with geological factors. With  
 57 the exception of inheritance, these factors yield ages that are  
 58 younger than the true age of the surface.

59 The  $^{10}\text{Be}$  ages for each landform are analysed using the mean  
 60 square of weighted deviates (MSWD; McDougall and Harrison,  
 1999) to assess whether they could statistically represent one

61 population or event, such as moraine stabilisation. Outliers are  
 62 removed iteratively from the dataset until the MSWD is  $\sim 1$  or  
 63 less. Samples from Lignite Creek (Ala-135–137 and 156), Healy  
 64 (Ala-157), Riley Creek 1 (Ala-15–20), Riley Creek 2 (Ala-120  
 65 and 121) landforms and the Reindeer Hills (Ala-158) and  
 66 Monahan Flat West (Ala-40–43, 145, 147 and 148) were  
 67 eliminated to identify strong age clusters. Scattered datasets that  
 68 do not pass MSWD analysis (i.e. less than three ages after  
 69 removal of outliers) were defined using principles of morphos-  
 70 stratigraphy. The impact of geological factors is likely small for  
 71 groups of boulders that pass MSWD analysis. One limitation of  
 72 the MSWD analysis is that clusters of ages that pass the test may  
 73 not necessarily represent the age of moraine deposition but  
 74 rather a postglacial erosional event.

## 75 Moraine successions

### 76 Nenana River valley

77 Landforms and previous work are discussed below in  
 78 stratigraphic order (oldest to youngest). Following a brief  
 79 description of the landforms associated with each ice limit, we  
 80 present our new  $^{10}\text{Be}$  age constraints.

### 81 Lignite Creek glaciation

82 Lignite Creek landforms and deposits are defined by a nearly  
 83 continuous moraine ridge with slopes of  $\sim 20^\circ$  and a crest that  
 84 rises  $\sim 30$  m above Panguingue Creek (Fig. 2). The moraine is  
 85 located north of Otto Lake and extends  $\sim 80$  km beyond the  
 86 contemporary snout of Yanert Glacier. South of Otto Lake and  
 87 in the glacial trough the moraine is discontinuous, covered  
 88 in frost-shattered rubble, and has occasional small angular  
 89 boulders. West of Otto Lake, granitic boulders are sparse and  
 90 the moraine crest is well vegetated with shrubs and trees.

91 Boulders on the crest (Ala-137A/B and 156) and the northern  
 92 slopes (Ala-135 and 136) of the moraine were sampled for  
 93  $^{10}\text{Be}$  dating. Boulder samples from the Lignite moraine have  
 94  $^{10}\text{Be}$  ages that range from  $13.4 \pm 1.8$  to  $103.9 \pm 8.2 \times \text{ka}^{\text{Q6}}$   
 95 (Fig. 4 and Table 2). These scattered ages do not pass MSWD  
 96 analysis.

97 The Stampede Gravel Pit ( $63.88811^\circ \text{N}$ ,  $149.10228^\circ \text{W}$ ),  
 98 located in the moraine north of Otto Lake, comprises stratified  
 99 gravel and tephra (Stampede Tephra), and is capped by  $\sim 35$  cm  
 100 of loess and overlain by fill (supporting information, Fig. 3SI;  
 101 Begét and Keskinen, 1991). The Stampede Tephra has been  
 102 correlated using major oxide concentrations in glass separates  
 103 found in eastern Beringia and the upper Cook Inlet (Reger *et al.*,  
 104 1996; Begét, 2001). Reger *et al.* (1996) reported two ages  
 105 with  $1\sigma$  error ( $175 \pm 12$  ka and  $181 \pm 19$  ka) for the tephra in the  
 106 Cook Inlet using TL methods on loess. Begét (2001) determined  
 107 a  $^{40}\text{Ar}/^{39}\text{Ar}$  age with  $1\sigma$  error of  $378 \pm 67$  ka on the tephra, but  
 108 he suspected that the tephra age was overestimated due to  
 109 contamination by older feldspar within the tephra. TL dating  
 110 provides a maximum age of ca. 180 ka for the Lignite Creek  
 111 glaciation, which Begét and Keskinen (1991) suggested to have  
 112 occurred ca. 140 ka or earlier.

113  $^{10}\text{Be}$  depth profile samples (Ala-201–205) were collected  
 114 from a 2 m deep pit in the moraine at Stampede Gravel Pit  
 115 (supporting information, Fig. 3SI), yielding a minimum age of  
 116 78 ka. Corrections for the  $\sim 35$  cm thick loess cover, transient  
 117 loess cover and surface erosion would increase the modelled  
 118 age.

**Table 2** Sample location, description and <sup>10</sup>Be terrestrial cosmogenic nuclide data and ages

Sample Name	Latitude (°N)	Longitude (°E)	Elevation (m a.s.l.)	Thickness (cm)	Boulder size length/width/ height (m)	Shielding correction	Quartz (g)	Be carrier (g)	Uncorrected <sup>10</sup> Be ± error 10 <sup>4</sup> atoms g <sup>-1</sup>	Corrected <sup>10</sup> Be ± error 10 <sup>4</sup> atoms g <sup>-1</sup>	PRIME Lab		CRONUS	
											Age std (ka) <sup>a</sup>	Age KN (ka) <sup>b</sup>	Age std (ka) <sup>c</sup>	Age KN (ka) <sup>b</sup>
<i>Carlo event</i>														
Ala-126A	63.610	148.777	682	2	2.2/1.3/0.9	1	19.2747	0.9446	15.06 ± 1.91	13.56 ± 1.72	16.0 ± 2.3	16.0 ± 2.3	15.0 ± 2.3	15.0 ± 2.3
Ala-126B	63.610	148.777	682	2	2.2/1.3/0.9	1	19.1700	0.9500	14.44 ± 1.82	13.01 ± 1.64	15.3 ± 2.2	15.3 ± 2.2	14.4 ± 2.2	14.4 ± 2.2
Ala-127	63.606	148.799	672	5	0.9/0.7/0.3	1	20.8284	0.9509	19.77 ± 2.84	17.80 ± 2.56	21.8 ± 3.5	21.8 ± 3.5	20.4 ± 3.4	20.4 ± 3.4
Ala-128	63.605	148.799	673	5	1.1/0.5/0.2	1	24.0809	0.9490	14.44 ± 1.53	13.01 ± 1.37	15.9 ± 2.0	15.9 ± 2.0	14.9 ± 2.0	14.9 ± 2.0
Ala-130	63.603	148.800	670	4	2.2/1.5/0.6	1	16.2974	1.0498	12.24 ± 2.16	11.02 ± 1.95	13.4 ± 2.5	13.4 ± 2.5	12.5 ± 2.5	12.5 ± 2.5
Ala-132	63.599	148.799	695	5	1.1/1.0/0.2	1	18.9043	0.9627	15.82 ± 2.32	14.25 ± 2.09	17.1 ± 2.8	17.1 ± 2.8	15.9 ± 2.7	15.9 ± 2.7
Ala-133	63.598	148.799	685	5	4.5/4.5/0.8	1	23.0005	0.9589	12.67 ± 3.83	11.41 ± 3.45	13.8 ± 4.3	13.8 ± 4.3	12.9 ± 4.1	12.9 ± 4.1
Ala-134	63.597	148.799	675	5	2.4/1.6/1.2	1	18.8999	0.9856	15.21 ± 1.97	13.70 ± 1.77	16.7 ± 2.4	16.7 ± 2.4	15.6 ± 2.4	15.6 ± 2.4
<i>Riley Creek 2 event</i>														
Ala-119	63.675	148.842	612	4	1.7/1.3/1.5	1	19.1576	0.9645	10.1 ± 1.53	9.10 ± 1.38	11.6 ± 1.9	11.6 ± 1.9	10.9 ± 1.9	10.9 ± 1.9
Ala-120	63.675	148.842	605	5	1.4/0.6/0.3	1	22.1545	0.9356	51.67 ± 6.96	46.54 ± 6.27	61.0 ± 9.3	61.0 ± 9.3	57.3 ± 9.3	57.3 ± 9.3
Ala-121	63.676	148.841	618	5	2.6/2.0/1.6	1	18.5902	0.9641	17.65 ± 2.37	15.90 ± 2.13	20.4 ± 3.1	20.4 ± 3.1	19.1 ± 3.1	19.1 ± 3.1
Ala-122	63.701	148.872	575	3	1.2/0.8/0.3	1	20.3712	0.9834	10.2 ± 3.00	9.19 ± 2.70	12.0 ± 3.6	12.0 ± 3.6	11.3 ± 3.5	11.3 ± 3.5
Ala-123	63.699	148.886	611	5	2.7/1.9/0.5	1	19.0683	0.9337	7.76 ± 2.40	6.99 ± 2.16	9.0 ± 2.8	9.0 ± 2.8	8.4 ± 2.7	8.4 ± 2.7
<i>Riley Creek 1 event</i>														
Ala-15	63.736	148.893	529	2	0.9/0.9/0.45	1	24.2305	0.2596	0.70 ± 0.07	0.63 ± 0.07	0.9 ± 0.1	0.9 ± 0.1	0.8 ± 0.1	0.8 ± 0.1
Ala-16	63.736	148.893	509	2	3.3/2.9/1.0	1	20.9488	0.9276	7.91 ± 1.32	7.12 ± 1.19	9.8 ± 1.8	9.8 ± 1.8	9.3 ± 1.7	9.3 ± 1.7
Ala-18	63.735	148.894	524	2	0.6/0.45/0.3	1	42.3903	0.9200	5.95 ± 1.06	5.36 ± 0.96	7.3 ± 1.4	7.3 ± 1.4	6.9 ± 1.4	6.9 ± 1.4
Ala-19	63.735	148.895	526	2	0.8/0.7/0.5	1	11.5411	0.9431	7.00 ± 3.46	6.31 ± 3.12	8.5 ± 4.3	8.5 ± 4.3	8.1 ± 4.1	8.1 ± 4.1
Ala-20	63.735	148.894	530	2	0.5/0.5/0.3	1	40.4180	0.2563	0.83 ± 0.08	0.75 ± 0.07	1.0 ± 0.1	1.0 ± 0.1	1.0 ± 0.1	1.0 ± 0.1
<i>Healy</i>														
Ala-11	63.845	149.034	579	3	1.1/6/0.2	1	24.4095	0.9483	40.21 ± 2.42	36.21 ± 2.18	47.6 ± 4.3	47.6 ± 4.3	44.8 ± 4.8	44.8 ± 4.8
Ala-12	63.848	149.025	568	2	2.1/1.4/1.0	1	36.1915	0.9040	46.34 ± 3.70	41.74 ± 3.33	55.0 ± 5.8	55.0 ± 5.8	51.8 ± 6.2	51.8 ± 6.2
Ala-13	63.848	149.025	568	2	1.8/1.2/0.4	1	25.4757	0.9122	45.35 ± 3.41	40.84 ± 3.07	53.8 ± 5.5	53.8 ± 5.5	50.7 ± 5.9	50.7 ± 5.9
Ala-23	63.834	149.000	579	2	1.5/1.2/0.6	1	35.2866	0.9126	50.12 ± 3.06	45.14 ± 2.76	59.0 ± 5.4	59.0 ± 5.4	55.5 ± 6.0	55.5 ± 6.0
Ala-24	63.833	149.000	574	2	2.9/1.6/0.5	1	33.0803	0.9440	47.47 ± 3.28	42.75 ± 2.96	56.1 ± 5.5	56.1 ± 5.5	52.8 ± 5.9	52.8 ± 5.9
Ala-25	63.834	149.001	576	2	1.3/1.0/0.7	1	21.2958	0.8983	50.22 ± 2.34	45.23 ± 2.11	59.2 ± 4.9	59.2 ± 4.9	55.8 ± 5.6	55.8 ± 5.6
Ala-107	63.837	148.978	595	4	1.5/1.0/1.1	1	21.1133	1.0112	48.01 ± 2.30	43.24 ± 2.07	56.6 ± 4.7	56.6 ± 4.7	53.2 ± 5.4	53.2 ± 5.4
Ala-108	63.834	148.975	601	3	2.3/1.5/0.5	1	26.0614	0.9449	45.39 ± 2.01	40.88 ± 1.81	52.7 ± 4.3	52.7 ± 4.3	49.6 ± 4.9	49.6 ± 4.9
Ala-157	63.855	149.043	558	5	2.4/1.7/0.7	1	19.2702	0.9416	23.10 ± 2.39	20.80 ± 2.15	28.2 ± 4.0	28.2 ± 4.0	26.6 ± 3.6	26.6 ± 3.6
<i>Lignite Creek</i>														
Ala-135	63.897	149.117	524	3	2.9/1.5/1	1	24.4290	0.9266	10.88 ± 1.29	9.80 ± 1.16	13.4 ± 1.8	13.4 ± 1.8	12.7 ± 1.9	12.7 ± 1.9
Ala-136	63.897	149.124	525	3	2.3/1.6/0.4	1	14.7533	0.9771	13.02 ± 2.22	11.73 ± 2.00	16.0 ± 3.0	16.0 ± 3.0	15.2 ± 2.9	15.2 ± 2.9
Ala-137A	63.865	149.132	644	3	8/7.5/5.8	1	17.0761	0.9753	69.77 ± 2.84	62.84 ± 2.55	78.6 ± 6.3	78.6 ± 6.3	73.6 ± 7.2	73.6 ± 7.2
Ala-137B	63.865	149.132	644	3	8/7.5/5.8	1	18.2945	0.9679	91.64 ± 3.48	82.54 ± 3.14	103.9 ± 8.2	103.9 ± 8.2	97.3 ± 9.5	97.3 ± 9.5
Ala-156	63.868	149.130	626	4	1.9/1.5/1.1	1	26.5345	0.9596	40.73 ± 2.18	36.68 ± 1.96	46.6 ± 4.0	46.6 ± 4.0	43.7 ± 4.5	43.7 ± 4.5

(Continues)

1  
2  
3  
4  
5  
6  
7  
8  
9  
10  
11  
12  
13  
14  
15  
16  
17  
18  
19  
20  
21  
22  
23  
24  
25  
26  
27  
28  
29  
30  
31  
32  
33  
34  
35  
36  
37  
38  
39  
40  
41  
42  
43  
44  
45  
46  
47  
48  
49  
50  
51  
52  
53  
54  
55  
56  
57  
58  
59  
60

61  
62  
63  
64  
65  
66  
67  
68  
69  
70  
71  
72  
73  
74  
75  
76  
77  
78  
79  
80  
81  
82  
83  
84  
85  
86  
87  
88  
89  
90  
91  
92  
93  
94  
95  
96  
97  
98  
99  
100  
101  
102  
103  
104  
105  
106  
107  
108  
109  
110  
111  
112  
113  
114  
115  
116  
117  
118  
119  
120

Table 2 (Continued)

Sample Name	Latitude (°N)	Longitude (°E)	Elevation (m a.s.l.)	Thickness (cm)	Boulder size length/width/ height (m)	Shielding correction	Quartz (g)	Be carrier (g)	Corrected		PRIME Lab		CRONUS Age std (ka) <sup>c</sup>
									<sup>10</sup> Be ± error 10 <sup>4</sup> atoms g <sup>-1</sup>	<sup>10</sup> Be ± error 10 <sup>4</sup> atoms g <sup>-1</sup>	Age std (ka) <sup>a</sup>	Age KN (ka) <sup>b</sup>	
<i>Reindeer Hills</i>													
Ala-151	63.404	148.843	1108	3	2.7/1.2/0.5	1	16.4951	1.0329	15.84 ± 2.93	13.2 ± 2.6	13.2 ± 2.6	13.2 ± 2.6	12.0 ± 2.5
Ala-152	63.403	148.843	1109	5	1.5/1.2/0.3	1	18.5325	0.9833	16.24 ± 1.86	13.7 ± 1.8	13.7 ± 1.8	13.7 ± 1.8	12.5 ± 1.8
Ala-153	63.401	148.847	1034	4	1.4/1.1/0.6	0.999	17.6738	0.9667	17.28 ± 1.88	15.5 ± 2.0	15.5 ± 2.0	15.5 ± 2.0	14.1 ± 2.0
Ala-154	63.401	148.840	1032	5	0.8/0.7/0.4	0.999	16.6285	0.9703	15.64 ± 1.92	14.1 ± 2.0	14.1 ± 2.0	14.1 ± 2.0	12.9 ± 1.9
Ala-155	63.400	148.847	1023	5	0.9/0.9/0.4	0.999	16.9683	0.9551	16.11 ± 1.92	14.7 ± 2.0	14.7 ± 2.0	14.7 ± 2.0	13.4 ± 2.0
Ala-158	63.402	148.858	972	5	2.5/1.0/0.8	1	24.1810	0.9384	12.93 ± 1.17	12.2 ± 1.4	12.2 ± 1.4	12.2 ± 1.4	11.2 ± 1.4
Ala-159	63.401	148.858	965	4	1.5/1.4/0.7	1	12.5970	0.9528	17.91 ± 2.36	16.9 ± 2.5	16.9 ± 2.5	16.9 ± 2.5	15.6 ± 2.5
Ala-160	63.401	148.858	964	5	1.3/0.8/0.3	1	17.0009	0.9597	18.99 ± 4.34	18.1 ± 4.3	18.1 ± 4.3	18.1 ± 4.3	16.7 ± 4.1
Ala-161	63.899	148.866	914	5	2.1/1.9/0.6	1	21.4909	0.9335	17.07 ± 3.21	17.0 ± 3.4	17.0 ± 3.4	17.0 ± 3.4	15.6 ± 3.3
Ala-162	63.899	148.866	915	4	2.0/1.6/0.4	1	17.7570	0.9703	13.82 ± 2.41	13.6 ± 2.5	13.6 ± 2.5	13.6 ± 2.5	12.5 ± 2.4
Ala-164	63.893	148.860	875	3	1.4/0.8/0.2	1	15.3558	1.0011	16.68 ± 3.46	16.8 ± 3.7	16.8 ± 3.7	16.8 ± 3.7	15.6 ± 3.5
Ala-165	63.893	148.860	869	4	1.8/1.6/0.4	1	19.2060	0.9673	14.00 ± 1.90	14.3 ± 2.2	14.3 ± 2.2	14.3 ± 2.2	13.2 ± 2.1
Ala-166	63.893	148.860	869	3	2.8/2.5/0.7	1	20.2669	0.9749	17.04 ± 3.70	17.3 ± 3.9	17.3 ± 3.9	17.3 ± 3.9	16.0 ± 3.8
<i>Monahan Flat West</i>													
Ala-40	63.306	148.210	863	2	1.8/1.3/1.1	1	36.1170	0.2537	1.59 ± 0.15	1.6 ± 0.2	1.6 ± 0.2	1.6 ± 0.2	1.5 ± 0.2
Ala-41	63.303	148.211	898	2	1.5/1.2/0.7	1	21.9314	0.2518	1.28 ± 0.13	1.3 ± 0.1	1.3 ± 0.1	1.3 ± 0.1	1.2 ± 0.2
Ala-42	63.302	148.210	897	2	1.8/1.3/1.1	1	14.5000	0.2645	1.80 ± 0.15	1.8 ± 0.2	1.8 ± 0.2	1.8 ± 0.2	1.6 ± 0.2
Ala-43	63.302	148.205	879	5	2.5/2.5/0.7	1	37.3237	0.8887	12.65 ± 1.07	12.9 ± 1.4	12.9 ± 1.4	12.9 ± 1.3	12.0 ± 1.5
Ala-145	63.306	148.212	859	5	1.5/0.9/0.8	1	15.7460	1.0065	22.11 ± 2.21	23.0 ± 2.8	23.0 ± 2.8	23.0 ± 2.7	21.3 ± 2.8
Ala-147	63.305	148.210	856	3	1.7/1.4/0.7	1	18.6074	0.9979	15.77 ± 1.74	16.2 ± 2.1	16.2 ± 2.1	16.2 ± 2.0	15.0 ± 2.1
Ala-148	63.305	148.210	855	5	1.7/1.1/0.6	1	19.0840	0.9910	31.99 ± 2.24	33.6 ± 3.3	33.6 ± 3.3	33.6 ± 3.1	31.0 ± 3.5
<i>Monahan Flat East</i>													
Ala-140	63.238	147.778	945	3	4.6/3.5/2.6	1	17.3510	1.0255	14.29 ± 1.81	13.6 ± 2.0	13.6 ± 2.0	13.6 ± 2.0	12.5 ± 1.9
Ala-141	63.238	147.777	936	3	1.8/1.6/0.9	1	18.1380	1.0074	13.77 ± 1.64	13.2 ± 1.8	13.2 ± 1.8	13.2 ± 1.8	12.2 ± 1.8
Ala-143	63.238	147.774	949	4	1.6/1.5/0.6	1	15.8586	1.0061	13.39 ± 1.78	12.8 ± 1.9	12.8 ± 1.9	12.8 ± 1.9	11.8 ± 1.9

Assume zero erosion rate, standard pressure and  $\rho = 2.7 \text{ g cm}^{-3}$  for all samples.

<sup>a</sup> Ages calculated using scaling model of Stone (2000) scaling scheme.

<sup>b</sup> Ages calculated using scaling model of Nishizumi<sup>et al.</sup> (1989) scaling scheme.

<sup>c</sup> Ages calculated using calibration KNSTD.

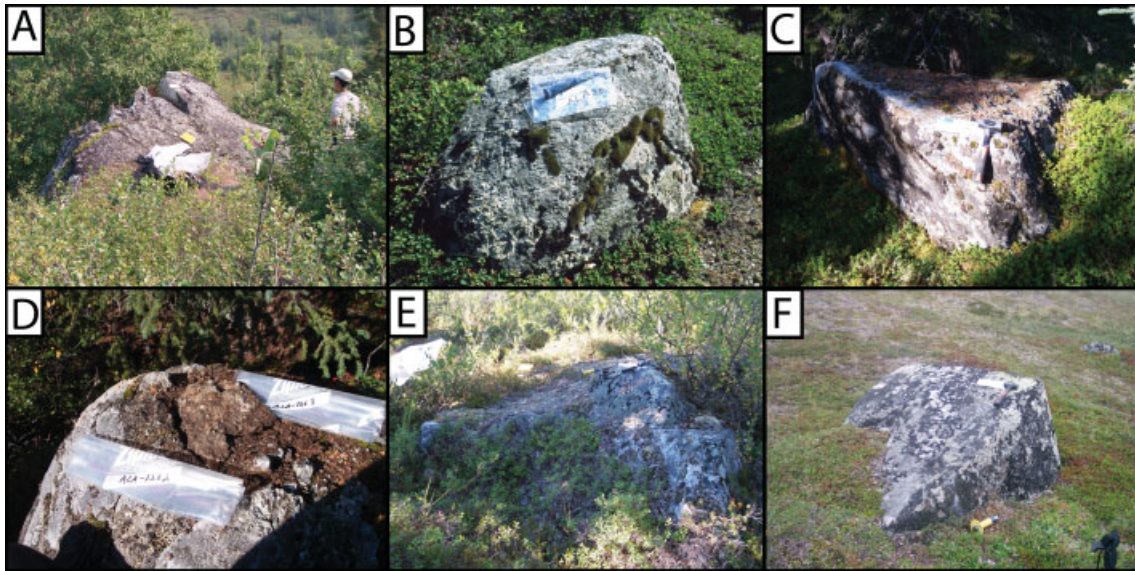


**Figure 3** Typical boulders in the Nenana valley. (A) Sample Ala-137A/B from large 8 m granitic boulder from the Lignite creek Moraine. (B) Sample Ala-25 (1.3 m) from a soft boulder on top of a Healy age drumlin. (C) Large 2.6 m granitic boulder (Ala-121) with a hard surface from the Riley creek moraine. (D) Differential weathering of a 2.2 m soft boulder (Ala-126A/B) located on the Carlo event moraine. (E) Sample Ala-133 from boulder with a hard surface located on the Carlo moraine. (F) Hard 1.5 m surfaced boulder (Ala-159) located on a glacial bench on Reindeer Hills

depth profile <sup>10</sup>Be age and would add a significant error to the age. Moreover, surficial processes including denudation and weathering, which clearly affected <sup>10</sup>Be boulder ages, likely affected the surface of the moraine as well.

Inheritance of the oldest moraine boulder (Ala-137B at 104 ka) is not likely because the old age is in agreement with the

minimum depth profile age (>78 ka), which could easily correlate with Ala-137B if the contemporary loess cover is taken into account. Sample Ala-137B may have a complex exposure history due to boulder surface erosion and exhumation; however, it is the best minimum approximation for the Lignite Creek glaciation. Using the oldest boulder (Ala-137B at

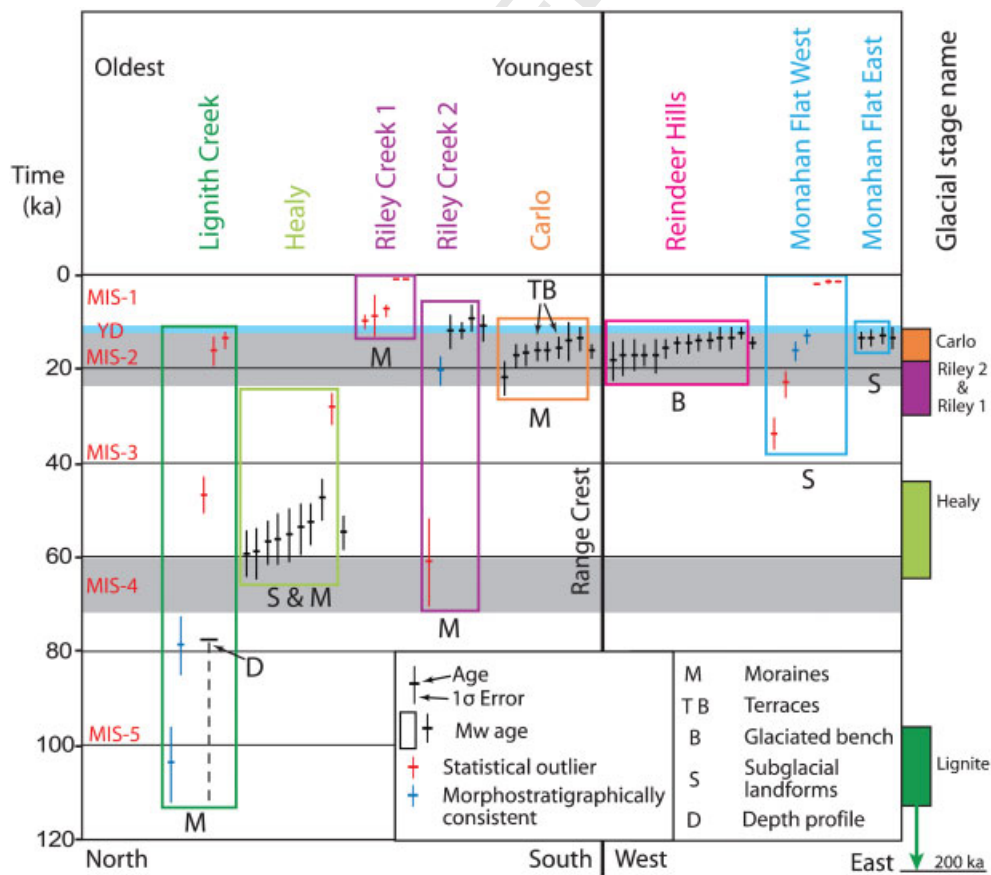


**Figure 4** <sup>10</sup>Be ages grouped by landform. The landforms are arranged in morphostratigraphic order, with the oldest (Teklankia) on the left and the youngest (Monahan Flat) on the right. <sup>10</sup>Be ages for boulders in each glacial stage are arranged in order of decreasing age. Erosion is not accounted for in the <sup>10</sup>Be ages. The ages shown in red were identified as outliers through MSWD analysis and were not included in *M<sub>w</sub>* ages. Ages shown in blue are from scattered datasets and follow morphostratigraphic order

104 ka) and the oldest TL age of Reger *et al.* (1996;  $181 \pm 19$  ka) as a maximum age constraint, the Lignite Creek glaciation likely occurred between ca. 104 and ca. 180 ka, which overlaps with MIS 5 and 6. Therefore we suggest that the Lignite Creek glaciation is a separate advance from the Healy glaciation, supporting the view of Begét (2001).

#### Healy glaciation

The Healy glaciation is represented by a nearly continuous laterofrontal moraine complex  $\sim 70$  km from the contemporary snout of Yanert Glacier (Fig. 2). The moraine consists of 10 individual ridges. The main (outermost) ridge has a crest that is 10–20 m wide with slopes of  $\leq 30^\circ$ . The Healy glacial advance represents the last time ice advanced out of the Nenana glacial trough into the foreland. Thorson and Hamilton (1976), Thorson (1986) and Begét and Keskinen (1991) suggested that the Healy glaciation should be assigned to MIS 4 or 6. However, there was no previous numerical age control for this glaciation.

Only four glacial boulders were found on the Healy moraine; these were sampled for  $^{10}\text{Be}$  dating (Ala-11–13 and 157). The condition of these boulders ranges from weathered boulders with weathering pits, weathering rinds, granular disintegration and soft surfaces to fresh boulders with clean, sharp fractures (supporting information, Table 1SI). Five additional samples were collected from Antenna Hill, which is located 3 km southeast of Otto Lake and inside the Healy glaciation limit. Samples were collected from the glacially eroded bedrock (Ala-107 and 108) and boulders on drumlins (Ala-23–25) on Antenna Hill. The boulders sampled on the drumlins have millimetre-deep weathering pits, centimetre-thick weathering rinds and are undergoing granular disintegration, whereas the bedrock samples were dominantly frost shattered.

A total of nine  $^{10}\text{Be}$  ages on Healy landforms range from  $28.2 \pm 4.0$  to  $59.0 \pm 5.1$  ka (Fig. 4; Table 2). Moraine boulders (Ala-11–13 and 157) have  $^{10}\text{Be}$  ages that range from  $28.2 \pm 4.0$  to  $55.0 \pm 5.8$  ka, whereas samples collected from drumlins on Antenna Hill (Ala-23–25) have  $^{10}\text{Be}$  ages between  $56.1 \pm 5.5$  and  $59.0 \pm 5.1$  ka. Bedrock samples (Ala-107 and 108) have ages of  $56.6 \pm 4.7$  and  $52.7 \pm 4.3$  ka, respectively. After the removal of one outlier (Ala-157;  $28.2 \pm 4.0$  ka), the Healy age boulders have a weighted mean ( $M_w$ ) age of  $54.6 \pm 3.5$  ka with an MSWD indicator of 0.58. We use the  $M_w$  of  $54.6 \pm 3.5$  ka as the minimum age for stabilisation of the Healy moraine.

Previous to our study, it was not known whether the Lignite Creek Moraine belonged to the Healy glaciation or if it was a separate glaciation (Wahrhaftig, 1958; Thorson and Hamilton, 1976; Ten Brink and Waythomas, 1985; Thorson, 1986; Begét and Keskinen, 1991). Our field observations support the view of Thorson and Hamilton (1976), Thorson (1986) and Begét and Keskinen (1991) that the Lignite Creek ridge is a moraine. Only a minimum age (104 ka) was determined for the Lignite Creek moraine, whereas ages on Healy landforms cluster at  $54.6 \pm 3.5$  ka. These  $^{10}\text{Be}$  ages support the view that the Lignite Creek is a distinct separate advance from the Healy glaciation.

#### Riley Creek 1

The Riley Creek 1 terminal moraine is located at the southern end of the glacial trough (Fig. 2; Thorson and Hamilton, 1976). Based on radiocarbon dating of wood in loess deposits on the Riley Creek 1 terrace, Hamilton (1982), Thorson (1986) and

Begét and Keskinen (1991) suggested that the Riley Creek 1 phase of the late Wisconsin glaciation occurred between 12 and  $25 \text{ }^{14}\text{C}$  ka BP (ca. 14–30 cal. ka BP; calibrated using CalPal<sup>1</sup>).

Most of the Riley Creek 1 terminal moraine has been significantly affected by erosion. However, lateral moraine remnants, hummocky moraine, glacial boulders and ice marginal drainages are still preserved (Thorson and Hamilton, 1976). The lateral moraine surface slopes northwards towards the Nenana River at  $\sim 10\text{--}15^\circ$ . The low slope angles, compared to the older moraines in the Nenana River valley, suggest that a significant amount of erosion has occurred since its formation (Thorson and Hamilton, 1976).

Five boulders (Ala-15, 16, 18, 19 and 20) were sampled for  $^{10}\text{Be}$  dating from the surface of hummocky moraine, yielding  $^{10}\text{Be}$  ages that range from ca.  $0.9 \pm 0.1$  to  $9.8 \pm 1.8$  ka (Fig. 4 and Table 2). These ages do not pass MSWD analysis; therefore we could not determine a numerical age for this moraine based on  $^{10}\text{Be}$  dating. The Riley Creek 1 ages likely reflect erosion and exhumation of boulders after early stabilisation of the moraine, and is consistent with the view of Wahrhaftig (1958) and Thorson (1986) that this moraine has been significantly eroded since deposition. However, we can define its age as between 30 cal. ka BP and the Carlo Creek event (see below) at  $16.0 \pm 1.8$  ka (Hamilton, 1982; Thorson, 1986; Begét and Keskinen, 1991).

#### Riley Creek 2

Wahrhaftig (1958) and Thorson and Hamilton, (1976) described a composite moraine south of the Riley Creek 1 phase ice limit that defines the limit of the Riley Creek 2 phase (Fig. 2). The moraine comprises till and gravel deformed into a recumbent fold. The Riley Creek 2 moraine is a nearly continuous ridge that can be traced for  $>1$  km, rises between 20 and 55 m above the valley floor and has slopes of  $30\text{--}35^\circ$ . Hummocky ground moraine exists within the Riley Creek 2 limit.

Wahrhaftig (1958) cites a radiocarbon age of  $10\ 560 \pm 200 \text{ }^{14}\text{C}$  a BP ( $12\ 380 \pm 290$  cal. a BP) on peat within till that is overlain by lacustrine sediment. Wahrhaftig (1958) believed that the peat was deposited after the maximum extent of the Riley Creek 2 phase of the late Wisconsin glaciation, but before the melting of stagnant ice that was covered with till. Ten Brink and Waythomas (1985) provided a maximum radiocarbon age of  $13\ 500 \pm 420 \text{ }^{14}\text{C}$  a BP ( $16\ 380 \pm 760$  cal. a BP) from plant debris in ice-dammed lake sediments under the Riley Creek 2 moraine. Therefore previous studies have constrained the age of the Riley Creek 2 phase to be between ca. 16.4 and ca. 12.4 ka.

Five samples (Ala-119–123) for  $^{10}\text{Be}$  dating collected from boulders on the hummocky ground moraine of the Riley Creek 2 phase (Fig. 2) have  $^{10}\text{Be}$  ages ranging from  $9.0 \pm 2.8$  to  $61.0 \pm 9.1$  ka (Fig. 4 and Table 2). The boulders have an  $M_w$  of  $11.0 \pm 2.9$  ka with an MSWD indicator of 0.22 after removing two outliers (Ala-120 and 121). This age is within error of the radiocarbon chronology. However, the  $M_w$  age of the Riley Creek 2 phase presents a problem because it is not in morphostratigraphic agreement with the ages from the Carlo Creek phase of the late Wisconsin glaciation, Reindeer Hills and Monahan Flat (see below). We suggest that the 22  $^{10}\text{Be}$  ages from the Carlo Creek phase, Reindeer Hills and south-central Monahan Flat localities are a more robust chronology than the three clustered ages from the Riley Creek 2 moraine. We therefore interpret the young age cluster of Riley Creek 2

<sup>1</sup>All calibrated radiocarbon ages in this paper were calculated using CalPal (<http://www.calpal-online.de/index.html>)

boulders as evidence of significant landform erosion and/or boulder exhumation event rather than moraine stabilisation. We cannot confidently determine the age of the Riley Creek 2.

### Carlo Creek

The convex north shape of the Carlo Creek moraine in the Nenana River valley, ~5 km north of the town of Carlo, suggests that it was formed by ice that flowed north into the valley via the Nenana Corridor (Fig. 2; supporting information, Fig. 1S1). Wahrhaftig (1958) described this as ground moraine comprising hummock topography with numerous hollows. Ten Brink and Waythomas (1985) obtained a radiocarbon age of  $12\ 110 \pm 230$  <sup>14</sup>C a BP ( $14\ 200 \pm 390$  cal. a BP) on peat accumulation outside the limit of Carlo Creek drift, and minimum radiocarbon ages of  $9060 \pm 160$  and  $5830 \pm 130$  <sup>14</sup>C a BP ( $10\ 180 \pm 240$  and  $6650 \pm 150$  cal. a BP) from basal peat in kettle holes within the ice limit.

Eight samples were collected for <sup>10</sup>Be dating from boulders on Carlo Creek landforms: six from the moraine (Ala-127, 128, 130, 132–134) and two located on top of the Carlo Creek outwash terrace (Ala-126A/B). Boulders from the Carlo Creek have <sup>10</sup>Be ages that range between  $13.4 \pm 2.5$  and  $21.8 \pm 3.4$  ka and an *M<sub>w</sub>* age of  $16.0 \pm 1.8$  ka with an MSWD indicator of 0.56 (Fig. 4). We use the *M<sub>w</sub>* to define the age for the Carlo Creek phase at  $16.0 \pm 1.8$  ka.

The tight clustering of seven <sup>10</sup>Be ages from Carlo Creek landforms and the agreement of ages between two separate sampling sites, moraine and terrace boulders suggest that the *M<sub>w</sub>* age of  $16.0 \pm 1.8$  ka is likely a good age approximation of moraine and terrace deposition. The Carlo Creek age is also supported morphostratigraphically by ages for deglaciation from Reindeer Hills ( $14.3 \pm 1.3$  ka) and the Monahan Flat east site ( $13.2 \pm 2.2$  ka); see below.

### Reindeer Hills

The glacial benches on Reindeer Hills are covered with boulders. Wahrhaftig (1958) suggested that ice from the Nenana and West Fork glaciers covered all but the uppermost peaks of Reindeer Hills during the Last Glacial Maximum (LGM) (supporting information, Fig. 2S1). Samples were collected from fresh granitic boulders for <sup>10</sup>Be dating on all five benches. These include Ala-164–166 from bench 1 (lowest), Ala-161 and 162 from bench 2, Ala-158–160 from bench 3, Ala-153–155 from bench 4 and Ala 151 and 152 from bench 5 (highest) (Table 2). The <sup>10</sup>Be ages range from ca.  $13 \pm x$  to  $19 \pm x$  ka<sup>Q7</sup> and there is no correlation between glacial bench position and <sup>10</sup>Be age. These boulders have an *M<sub>w</sub>* age of  $14.3 \pm 1.2$  ka with an MSWD indicator of 0.72 after the removal of one outlier (Ala 158;  $12.2 \pm 1.4$  ka). The overlap of <sup>10</sup>Be ages and the low MSWD indicate that these boulders represent one population corresponding to the deglaciation from the Reindeer Hills by  $14.3 \pm 1.2$  ka (supporting information, Fig. 2S1). This indicates that the Nenana Corridor must have been deglaciated by  $14.3 \pm 1.2$  ka.

### Monahan Flat

A series of roches moutonnées are located on the western edge ( $63.3^\circ$  N,  $148.2^\circ$  W) and the south-central part ( $63.2^\circ$  N,  $147.8^\circ$  W) of Monahan Flat (supporting information, Fig. 2S1).

Wahrhaftig (1958) suggested that ice from the Nenana and West Fork glaciers flowed through the basin and coalesced with glaciers in Broad Pass. Samples from the western end of Monahan Flat were collected from seven granitic boulders for <sup>10</sup>Be dating. These boulders were collected from atop roche moutonnées (supporting information, Fig. 2S1). The granitic erratics (Ala-40–43, 145, 147 and 148) at the western end of Monahan Flat have <sup>10</sup>Be ages that range from  $1.3 \pm 0.1$  to  $33.6 \pm 3.3$  ka (Figs<sup>Q8</sup> 2 and 8 and Table 2). These ages do not pass MSWD analysis, and therefore an age of deglaciation is not assigned. Three granitic erratics (Ala-140, 141, 143) from the south-central portion of the Monahan Flat have <sup>10</sup>Be ages between  $12.8 \pm 1.9$  and  $13.6 \pm 2.0$  ka (Fig. 4 and Table 2). These ages cluster and have an *M<sub>w</sub>* age of  $13.2 \pm 2.2$  ka with an MSWD value of 0.06.

### Observations of <sup>10</sup>Be dating on landforms and boulders

The number of outliers and age groups that failed MSWD analysis demonstrates the strong influence of geological processes on our <sup>10</sup>Be ages. Our success seems to depend largely on the landform type that was sampled. For example, the <sup>10</sup>Be ages from erratics on Healy age drumlins are more tightly clustered than boulders on Healy moraines. Collecting samples from landforms in addition to moraines may provide more reliable chronologies in central Alaska. Erosion, weathering and stability of landforms are probably the major factors in influencing the distribution of <sup>10</sup>Be ages on landforms studied here. Our data show that denudation of old (>60 ka) moraines such as the Lignite Creek moraines leads to exhumation of boulders and a large spread of <sup>10</sup>Be ages, which ultimately produces a significant underestimation of the true landform age.

We found little correlation between boulder surface texture, which reveals varying degrees of bedrock erosion of our sampled boulders, and <sup>10</sup>Be age (supporting information, Table 1S1). However, we did find that visible erosion of boulders has a significant impact on <sup>10</sup>Be ages in the range of 100–180 ka (Lignite Creek). This is revealed by samples Ala-137A ( $78.6 \pm 6.3$  ka) and 137B ( $103.9 \pm 8.2$  ka) that were collected from one boulder  $8 \times 7.5 \times 5.8$  m in size (Table 2; supporting information, Table 1S1). These results suggest that sample location on a boulder's surface may be as important as boulder selection when the landform is >60 ka. On the other hand, varying degrees of erosion visible on boulders from young landforms do not seem to significantly affect <sup>10</sup>Be age. Samples Ala-126A ( $16.0 \pm 2.3$  ka; collected from a solid surface) and 126B ( $15.3 \pm 2.2$  ka; collected from a loose chip inside a weathering pit) on the same boulder yielded ages within one standard deviation of each other.

Isotopic inheritance does not appear to be significant in our study area. Three outliers (Ala-120, 145 and 148) out of 55 samples were identified using MSWD analyses and morphostratigraphic limits. All three samples with identifiable inheritance were collected on young landforms (late Wisconsin). Geological processes such as bedrock weathering and landform degradation increase age uncertainties and make it difficult to identify inheritance on older landforms.

### Regional correlations

Correlating our glacial record with other regions in Alaska is challenging, particularly for the Lignite Creek glaciation, where

little geochronological data are available (Briner and Kaufman, 2008). To adequately compare the timing of glaciation, previously published  $^9\text{Be}/^{10}\text{Be}$  ratios from Balascio *et al.* (2005) and Briner *et al.* (2001, 2005) were converted to the revised ICN of Nishiizumi *et al.* (2007). Ages were calculated using the (PRIME) Laboratory Rock Age Calculator with the Lal (1991)/Stone (2000) scaling scheme.  $^{36}\text{Cl}$  ages were not recalculated and are for zero erosion. We did not make any correction for erosion when calculating the previously published  $^{10}\text{Be}$  ages. We use the chronostratigraphic interpretations of the original authors for all age determinations.

### Pre-late Wisconsin

There are few chronologies in Alaska on glacial landforms pre-dating the Wisconsin glaciation. The Delta River valley (~100 km east of the Nenana River valley), however, provides a useful comparison with our data. The age of the Delta glaciation is bracketed between  $140 \pm 10$  ka and  $190 \pm 20$  ka using tephrochronology and is correlated to MIS 6 (Begét and Keskinen, 2003). Our chronology (104–180 ka) for the Lignite Creek glaciation suggests that the Lignite Creek and Delta glaciation can be correlated.

### Early Wisconsin

The  $^{10}\text{Be}$  ages from the Healy glaciation range from 48 to 59 ka, after removing outliers, and have an  $M_w$  age of  $54.6 \pm 3.5$  ka. The Healy glaciation likely correlates with the Farewell I glacial stage of Briner *et al.* (2005) in the Swift River valley in the western Alaska Range. The Farewell I glacial stage has recalculated  $^{10}\text{Be}$  ages that range from  $45.5 \pm 3.6$  to  $57.2 \pm 4.2$  ka (supporting information, Table 2SI). Briner *et al.* (2005) determined a range of ages for the Farewell I glacial stage by calculating the age of the oldest boulder with a maximum ( $8 \text{ mm ka}^{-1}$ ) and minimum ( $4.8 \text{ mm ka}^{-1}$ ) erosion rate. The recalculated age of the oldest boulder uncorrected for erosion is  $57.2 \pm 3.9$  ka (supporting information, Table 2SI). This age overlaps with both the  $M_w$  age of  $54.6 \pm 3.5$  ka and oldest boulder (Ala-25) age of  $59.2 \pm 4.6$  ka of the Healy glaciation. In the Ahklun Mountains, Briner *et al.* (2001) obtained four  $^{36}\text{Cl}$  ages to define the timing of Arolik Lake glaciation. The ages are not corrected for erosion and range from 58 to 64 ka. Briner *et al.* (2001) reported an  $M_w$  age of  $60.3 \pm 3.2$  ka, which overlaps with the age of the Healy glaciation ( $M_w$   $54.6 \pm 3.5$  ka). The overlap of three chronologies in the Alaska Range and Ahklun mountains suggests that deglaciation from a significant phase of glaciation in the early Wisconsin occurred during earliest MIS 3 to Late MIS 4 in Alaska.

### Late Wisconsin

The Carlo Creek ages range from 13 to 22 ka, after removing outliers, and have an  $M_w$  age of  $16.0 \pm 1.8$  ka. The Farewell II moraine of Briner *et al.* (2005) in the Swift River valley has recalculated  $^{10}\text{Be}$  ages that range from  $19.1 \pm 1.5$  to  $22.1 \pm 1.7$  ka. The Hubley Creek moraine in the Jago River valley, northeastern Brooks Range, has recalculated  $^{10}\text{Be}$  ages that range from  $16.3 \pm 1.8$  to  $22.6 \pm 2.5$  ka (BR02-1 to BR02-4; Balascio *et al.*, 2005; Briner *et al.*, 2005). Briner *et al.* (2005) determined a range of ages for the Farewell II and Hubley Creek moraines by calculating the age of the oldest boulder with a

maximum ( $8 \text{ mm ka}^{-1}$ ) and minimum ( $4.8 \text{ mm ka}^{-1}$ ) erosion rate. The recalculated ages of the oldest boulders for the Farewell II and Hubley Creek moraines uncorrected for erosion are  $22.1 \pm 1.7$  ka and  $22.6 \pm 2.5$  ka, respectively. These ages overlap with the oldest boulder (Ala-127) from the Carlo Creek phase ( $21.8 \pm 3.4$  ka) and the single reasonable age from the Riley Creek 2 phase (Ala-121 at  $20.4 \pm 3.1$  ka).

Briner *et al.* (2001) obtained 19  $^{36}\text{Cl}$  ages on the Kisogle, Cloud Lake, Chilly Valley and Gusty Lakes moraines to constrain the timing of the Klak Creek glaciation in the Ahklun Mountains. Briner *et al.* (2001) excluded outliers from the ultimate age determination, which is 17–19 ka, and 15–18 ka for the Kisogle and Cloud Lake moraines, respectively. The Kisogle moraine has an  $M_w$  of  $17.5 \pm 0.9$  ka and the Cloud Lake moraine has an  $M_w$  age of  $16.7 \pm 1.4$  ka. Briner *et al.*'s (2001) ages for the Chilly Valley and Gusty Lakes moraines range from 17 to 20 ka and from 18 to 21 ka, respectively. These ages have a mean and standard error of  $17.8 \pm 1.9$  ka and  $19.6 \pm 1.4$  ka for the Chilly Valley and Gusty Lakes moraines, respectively. The ages of the six moraines investigated by Balascio *et al.* (2005) and Briner *et al.* (2001, 2005) are in reasonable agreement with the age of the Carlo Creek phase ( $16.0 \pm 1.8$  ka).

### Conclusion

Defining the timing of glaciation in the central Alaska Range using  $^{10}\text{Be}$  dating is challenging because of the numerous geological processes affecting boulders and rock surfaces in the region.  $^{10}\text{Be}$  ages on boulders from drumlins and glacial benches cluster better than hummocky ground moraines and non-hummocky end moraines. There is no correlation between visible weathering on boulders and  $^{10}\text{Be}$  age. The position of boulders on the landscape, and type and age of landforms, seem to have a greater impact on  $^{10}\text{Be}$  age than boulder weathering. Despite these problems, landforms dating to the Wisconsin glaciation generally provide reasonable  $^{10}\text{Be}$  ages, with the exception of the Riley Creek phase moraines and Monahan Flat west. The Lignite Creek glaciation likely correlates with MIS 5 or 6 (Table 1). The Healy glaciation dates to  $54.6 \pm 3.5$  ka (early MIS 3) and represents a reasonable upper limit of  $^{10}\text{Be}$  dating in this region. The Carlo Creek phase landforms date to  $16.0 \pm 1.8$  ka. Morphostratigraphic position and previous radiocarbon dating brackets the Riley Creek 1 and 2 phases between 16 and 30 ka. Deglaciation of Reindeer Hills and Monahan Flat east occurred by  $14.3 \pm 1.3$  ka and  $13.2 \pm 2.2$  ka, respectively.

The correlation of moraines in several mountain belts across Alaska during both early last glacial and the LGM suggests that the region responded to climatic change synchronously. This synchronicity may be important when modelling current climate change and the response of glaciers across Alaska. Moreover, the  $16.0 \pm 1.8$  ka stabilisation age of the Carlo Creek phase supports the view of Briner *et al.* (2005) and Birner and Kaufman (2008) that late Wisconsin deglaciation in Alaska occurred during 17–21 ka. Our study highlights the usefulness of exposure dating methods in central Alaska and also illuminates the potential pit falls. The chronostratigraphy we have developed will provide a framework for future studies of palaeoenvironmental change and landscape evolution in central Alaska.

*Acknowledgements* Thanks to the Braun and Creig families, Jim Mehegen, Phil Brease, Lucy Tyrrell, Denali National Park, Tim Debey, James Brokaw, Dan Muhs, Susan Ma and the National Natural Science

Foundation of China (Project NSFC 40301004). We would also like to thank Drs Jason Briner and Greg Balco and two anonymous reviewers for constructive comments and discussions that greatly improved this study and paper.

## References

- Arendt AA, Echelmeyer KA, Harrison WD, Lingle CS, Valentine VB. 2002. Rapid wastage of Alaska glaciers and their contribution to rising sea level. *Science* **297**: 392–386.
- Balascio NL, Kaufman DS, Briner JP, Manley WF. 2005. Late Pleistocene glacial geology of the Okpilak–Kongakut Rivers region, northwestern Brooks Range, Alaska. *Arctic, Antarctic, and Alpine Research* **37**: 416–424.
- Balco G, Briner J, Finkel RC, Rayburn J, Ridge JC, Schaefer JM. 2008. Regional beryllium-10 production rate calibration for late-glacial northeastern North America. *Quaternary Science Reviews* **4**: 93–107.
- Begét JE. 2001. Continuous Late Quaternary proxy climate records from loess in Beringia. *Quaternary Science Reviews* **20**: 499–507.
- Begét JE, Keskinen J. 1991. The Stampede tephra: a middle Pleistocene marker bed in glacial and eolian deposits of central Alaska. *Canadian Journal of Earth Sciences* **28**: 991–1002.
- Begét JE, Keskinen MJ. 2003. Trace-element geochemistry of individual glass shards of the Old Crow tephra and the age of the Delta glaciation, central Alaska. *Quaternary Research* **60**: 63–69.
- Briner JP, Kaufman DS. 2008. Late Pleistocene mountain glaciation in Alaska: key chronologies. *Journal of Quaternary Science* **23**: 659–670.
- Briner JP, Swanson TW, Caffee MW. 2001. Late Pleistocene cosmogenic <sup>36</sup>Cl glacial chronology of the southwestern Ahklun Mountains, Alaska. *Quaternary Research* **56**: 148–154.
- Briner JP, Kaufman DS, Manley WF, Finkel RC, Caffee MW. 2005. Cosmogenic exposure dating of late Pleistocene moraine stabilization in Alaska. *Geologic Society of America Bulletin* **117**: 1108–1120.
- CalPal. 2007. [Cologne<sup>09</sup> radiocarbon calibration and paleoclimate research package](http://www.calpal-online.de/index.html). <http://www.calpal-online.de/index.html> [31 March 2010].
- Dortch JM, Owen LA, Haneberg WC, Caffee MW, Dietsch C, Kamp DU. 2009. Nature and timing of large-landslides in the Himalaya and Transhimalaya of northern India. *Quaternary Science Reviews* **28**: 1037–1054.
- Eberhart-Phillips D, Haeussler PJ, Freymueller JT, Frankel AD, Rubin CM, Craw P, Ratchkovski NA, Anderson G, Carver GA, Crone AJ, Dawson TE, Fletcher H, Hansen R, Harp EL, Harris RA, Hill DP, Hreinsdóttir S, Jibson RW, Jones LM, Kayen R, Keefer DK, Larsen CF, Moran SC, Personius SF, Plafker G, Sherrod B, Sieh K, Sitar N, Wallace WK. 2003. The 2002 Denali Fault earthquake, Alaska: a large magnitude, slip-partitioned event. *Science* **300**: 1113–1118.
- Evans DJE, Benn DI. 2004. *A Practical Guide to the Study of Glacial Sediments*. Arnold: London.
- Gosse JC, Phillips FM. 2001. Terrestrial in situ cosmogenic nuclides: theory and application. *Quaternary Science Reviews* **20**: 1475–1560.
- Hamilton TD. 1982. A late Pleistocene glacial chronology for the southern Brooks Range: stratigraphic record and regional significance. *Geologic Society of America Bulletin* **93**: 700–716.
- Hamilton TD, Thorson RM. 1983. The Cordilleran Ice Sheet in Alaska. In *Late Quaternary Environments of the United States*, Vol. I, Porter SC (ed.). University of Minnesota Press: Minneapolis, MN; 38–52.
- IPCC (Intergovernmental Panel on Climate Change). 2007. Working Group II. In *Climate Change Impacts, Adaptation and Vulnerability*; 653–686. <http://www.ipcc-wg2.org/> [31 March 2010].
- Kohl CP, Nishiizumi K. 1992. Chemical isolation of quartz for measurements of in-situ-produced cosmogenic nuclides. *Geochimica et Cosmochimica Acta* **56**: 3583–3587.
- Lal D. 1991. Cosmic ray labeling of erosion surfaces: in situ nuclide production rates and erosion models. *Earth and Planetary Science Letters* **104**: 424–439.
- LIGA members, working group for the study of the Last Interglacial in the Arctic and sub-Arctic. 1991. Report of the 1st discussion group: the Last Interglacial in high latitudes of the northern hemisphere: terrestrial and marine evidence. *Quaternary International* **10–12**: 9–28.
- Matmon A, Schwartz DP, Haeussler PJ, Finkel R, Lienkaemper JJ, Stenner HD, Dawson TE. 2006. Denali fault slip rates and Holocene–late Pleistocene kinematics of central Alaska. *Geological Society of America* **34**: 645–648.
- McDougall I, Harrison TM. 1999. *Geochronology and Thermochronology by the <sup>40</sup>Ar/<sup>39</sup>Ar Method*, (2nd edn). Oxford University Press: Oxford.
- Nishiizumi K, Imamura M, Caffee MW, Southon JR, Finkel RC, McAninch J. 2007. Absolute calibration of <sup>10</sup>Be AMS standards. *Nuclear Instruments and Methods in Physics Research – Beam Interactions with Materials and Atoms* **258B**: 403–413.
- PRIME Laboratory. 2007. PRIME Laboratory rock age calculator. <https://www.physics.purdue.edu/ams/rosetest/Rkversion1/rockpara.php> [31 March 2010].
- Reger RD, Pinney DS, Burk RM, Wiltse MA. 1996. Catalog and initial analyses of geologic data related to middle to late Quaternary deposits, Cook Inlet region, Alaska. *State of Alaska Division of Geological and Geophysical Surveys Report of Investigation*, Vol. 95–96, Fairbanks, AK.
- Ridgway KD, Trop JM, Nokleberg WJ, Davidson CM, Eastham KR. 2002. Mesozoic and Cenozoic tectonics of the eastern and central Alaska Range: progressive basin development and deformation in a suture zone. *Geological Society of America Bulletin* **114**: 1480–1504.
- Stone JO. 2000. Air pressure and cosmogenic isotope production. *Journal of Geophysical Research* **105**: 23753–23760.
- Ten Brink NW, Waythomas CF. 1985. Late Wisconsin glacial chronology of the north-central Alaska Range: a regional synthesis and its implications for early human settlements. In *North Alaska Range Early Man Project*, Swanson W (ed.). *National Geographic Society Research Reports* **19**: 15–32.
- Thorson RM. 1986. Late Cenozoic glaciation of the Nenana valley. In *Glaciation in Alaska: The Geologic Record*, Hamilton TD, Reed KM, Thorson RM (eds). Alaska Geological Society: Fairbanks, AK; 99–121.
- Thorson RM, Bender G. 1985. Eolian deflation by ancient katabatic winds: a late Quaternary example from the north Alaska Range. *Geologic Society of America Bulletin* **96**: 702–709.
- Thorson RM, Hamilton TD. 1976. Geology of the Dry Creek Site: a stratified early man site in interior Alaska. *Quaternary Research* **7**: 149–176.
- US Geological Survey. 2007. United States Geological Survey seamless data distribution system, earth resources observations and science (EROS). <http://seamless.usgs.gov/> [31 March 2010].
- Wahrhaftig C. 1958. Quaternary geology of the Nenana River valley and adjacent parts of the Alaska Range. *US Geological Survey Professional Paper* 293-A, Reston, VA.

## Author Query Form (JQS/1406)

**Special Instruction: Author please include responses to queries with your other corrections and return by e-mail.**

**Q1: Author: Hickman (1977) not on ref. list.**

**Q2: Author: Capps (1940) not on ref. list.**

**Q3: Author: Beget et al. (1991) not on ref. list.**

**Q4: Author: Nishiizumi (1989) not on ref. list.**

**Q5: Author: 'ICP/ICP-MS' – does this need to be given in full? (It might seem a little clumsy in full in this context.)**

**Q6: Author: '103.9±8.2x ka' OK?**

**Q7: Author: '13±x to 19±x ka' OK?**

**Q8: Author: 'Figs 2 and 8' – there is no Fig. 8.**

**Q9: Author: CalPal (2007) not cited in text.**

UNCORRECTED PROOFS

1	61
2	62
3	63
4	64
5	65
6	66
7	67
8	68
9	69
10	70
11	71
12	72
13	73
14	74
15	75
16	76
17	77
18	78
19	79
20	80
21	81
22	82
23	83
24	84
25	85
26	86
27	87
28	88
29	89
30	90
31	91
32	92
33	93
34	94
35	95
36	96
37	97
38	98
39	99
40	100
41	101
42	102
43	103
44	104
45	105
46	106
47	107
48	108
49	109
50	110
51	111
52	112
53	113
54	114
55	115
56	116
57	117
58	118
59	119
60	120